NJC

ROYAL SOCIETY OF CHEMISTRY

PAPER

View Article Online
View Journal | View Issue

Cite this: *New J. Chem.*, 2023, **47**, 5930

Synthesis and characterisation of group 11 metal complexes with a guanidine-tagged triphenylphosphine and evaluation of the isolated Au(I) complexes in gold-mediated organic reactions†

Zdeněk Leitner, Ivana Císařová and Petr Štěpnička *

Received 30th January 2023,
Accepted 16th February 2023

DOI: 10.1039/d3nj00451a

rsc.li/njc

Phosphines bearing guanidine substituents at the backbone are attractive hybrid ligands that have not yet received adequate attention. This paper describes group 11 metal complexes of a guanidine-substituted triphenylphosphine, *viz.*, *N*″-[2-(diphenylphosphino)phenyl]-*N*,*N*′-diisopropylguanidine (**1**). Reactions of **1** with Cu(I) and Ag(I) precursors yielded the P,N-chelate complexes [M(1-κ^2*P*,*N*)$_2$]X, where M/X = Cu/BF_4, Cu/Br, Ag/SbF_6 and Ag/Br. Conversely, reacting **1** and the hydrochloride **1**·HCl with [AuCl(SMe_2)] produced the corresponding phosphine complexes [AuCl(**1**-κ*P*)] and [AuCl(**1**H-κ*P*)]Cl, which were further converted into [{μ(P,N)-**1**}$_2$$Au_2$][$SbF_6$]$_2$ and [AuCl(**1**H-κ*P*)][SbF_6], respectively, by reacting with Ag[SbF_6]. These compounds and the bis-phosphine complex [Au(**1**-κ*P*)$_2$][SbF_6] were studied as precatalysts in the Au-mediated cyclisation of *N*-propargylbenzamide and the addition of benzoic acid across terminal alkynes. Of the Au(I)-**1** complexes studied, the complex [{μ(P,N)-**1**}$_2$$Au_2$][$SbF_6$]$_2$ was particularly attractive as a stable and well-defined, silver-free precatalyst, which can be conveniently activated *in situ* by the addition of a protic acid (either as an additive or a substrate).

Introduction

A particular combination of functional groups, whose properties can be widely varied through substituents, makes guanidine-substituted phosphines attractive hybrid donors. For instance, triphenylphosphine derivative **A** (Scheme 1) was studied as a supporting ligand in Re(I) complexes used to investigate the elementary steps of CO hydrogenation.[1] More recently, compound **B** was employed in platinum metal complexes, which were subsequently utilised in small molecule activation and indole nitroethylation.[2] Analogous phosphines bearing cyclic guanidine moieties, **C** and **D**, were evaluated as substrate-directing ligands in hydroformylation of β,γ-unsaturated carboxylic acids[3] and found to form highly active H/D-exchange iridium catalysts (type **E**).[4]

Recently, we prepared a series of ferrocene-based phoshinoguanidines **F** (Scheme 1) and studied their coordination behaviour,[5] demonstrating that the ligating properties of these donors can be substantially modified by changing the protonation state of their guanidine moiety.[6] We also focused on the analogous triphenylphosphine derivative **1** and described the protonation-dependent coordination properties of this compound in Pd(II) complexes.[7] Here, we extend our studies

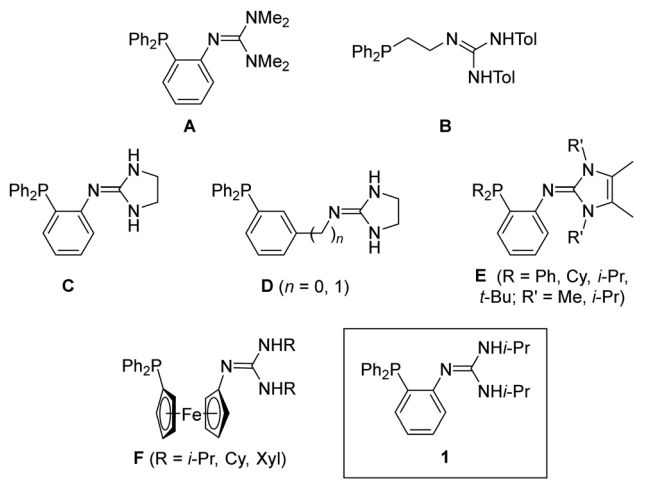

Scheme 1 Examples of phosphinoguanidine donors (Tol = 4-tolyl, Cy = cyclohexyl, Xyl = 2,6-dimethylphenyl).

Department of Inorganic Chemistry, Faculty of Science, Hlavova, 2030, 128 40 Prague, Czech Republic. E-mail: petr.stepnicka@natur.cuni.cz

† Electronic supplementary information (ESI) available: Additional structure diagrams, summary of relevant crystallographic parameters and copies of the NMR spectra. CCDC 2237665–2237672. For ESI and crystallographic data in CIF or other electronic format see DOI: https://doi.org/10.1039/d3nj00451a

focused on compound **1** further towards complexes with group 11 metals and further explore the catalytic properties of the prepared Au(I)-**1** complexes in gold-mediated organic transformations.

Results and discussion

Cu(I) and Ag(I) complexes

Initially, compound **1** was allowed to react with Cu(I) and Ag(I) precursors with weakly coordinating anions, such as $[Cu(MeCN)_4][BF_4]$ and $Ag[SbF_6]$ (Scheme 2). These reactions, performed at a 1 : 2 metal-to-ligand ratio in dichloromethane, proceeded similarly to produce the respective bis-chelate complexes **2a** and **3a**, which were isolated as air-stable, colourless solids with good yields (93% for **2a** isolated by precipitation and 70% for the crystallised complex **3a**). Analogous reactions with CuBr and AgBr proceeded similarly to give complexes **2b** and **3b**. In this case, the addition of ligand **1** to a suspension of the bromide salt resulted in the dissolution of the metal precursor and the formation of a colourless solution. The products were isolated by precipitation or crystallisation. As solids, however, the bromide salts were practically insoluble in common organic solvents, which precluded any analysis by common solution methods (*e.g.*, NMR spectroscopy). Notably, analogous reactions employing equimolar amounts of the starting materials yielded the same, $[M(\mathbf{1})_2]^+$-type products.

Complex formation was revealed in the ^{31}P NMR spectra. For **2a**, a broadened ^{31}P NMR signal was observed at δ_P −17.8, which is upfield from the free ligand (δ_P −13.8), while complex **3a** displayed a resonance at δ_P −5.5 that was split into a double doublet due to interactions with ^{107}Ag and ^{109}Ag ($^1J_{AgP}$ = 436 and 503 Hz, respectively). The ^1H NMR and ^{13}C NMR spectra displayed all expected signals. However, the ^{13}C NMR signals of the ^{31}P-coupled carbons were observed as virtual triplets due to virtual coupling in the ^{13}C–^{31}P–Pd–^{31}P–^{12}C AA′X-type spin systems[8] (in the case of **3a**, further splitting due to C–Ag interactions was observed). The presence of cations $[M(\mathbf{1})_2]^+$ (in solution) was verified by mass spectrometry using soft ionisation techniques (ESI or MALDI), and the sample purity was corroborated by elemental analysis. The latter methods were also used to characterise the insoluble compounds **2b** and **3b**.

The crystal structures of **2a**·$C_2H_4Cl_2$, **2b**·CH_2Cl_2 and **3a** were determined using X-ray diffraction analysis. Compound **3b** yielded only poor-quality crystals: the collected data allowed us to confirm the structure but not a satisfactory refinement.

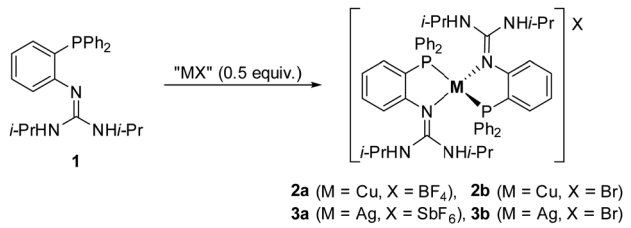

Scheme 2 Synthesis of Cu(I) and Ag(I) complexes with ligand **1**.

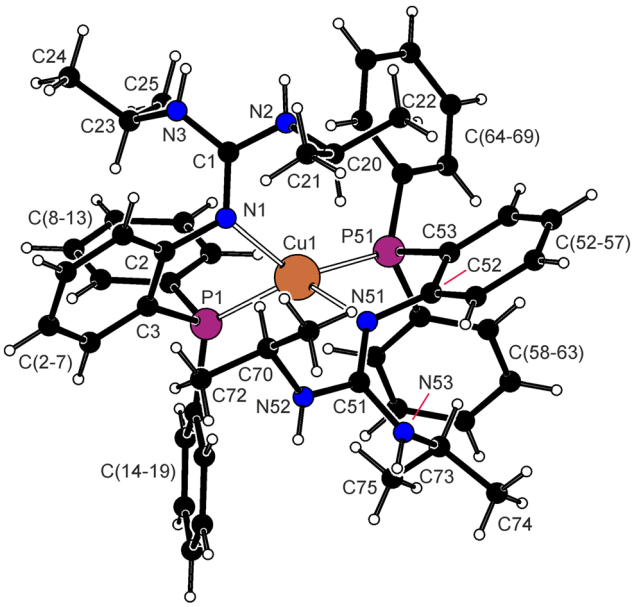

Fig. 1 View of the complex cation in the structure of **2b**·CH_2Cl_2.

The complex cations in the structures of **2a**·$C_2H_4Cl_2$, **2b**·CH_2Cl_2 and **3a** are generally similar. A structure diagram of the representative compound **2b** is shown in Fig. 1, and the remaining structures are presented in the ESI.† The geometric data are summarised in Table 1.

The coordination spheres in **2a**·$C_2H_4Cl_2$, **2b**·CH_2Cl_2 and **3a** are distorted not only due to varying M-donor distances but also severely twisted. While the M–P bond lengths do not change much in the entire series, the M–N distances vary more, presumably due to steric factors and a lower covalence of the M–N dative bonds.[9]

The P–M–N angles associated with the chelate rings are significantly narrower (72–83° in the series) than the remaining interligand angles, reflecting the size and rigidity of the 1, 2-phenylene backbone. Only the N–M–N′ angles remain close to

Table 1 Selected distances and angles for **2a**·$C_2H_4Cl_2$, **2b**·CH_2Cl_2 and **3a** (in Å and deg)

Parameter[a]	**2a**·$C_2H_4Cl_2$[b]	**2b**·CH_2Cl_2	**3a**
M	Cu	Cu	Ag
M–P	2.240(1)	2.2392(7)/2.2366(7)	2.401(1)/2.418(1)
M–N	2.121(2)	2.126(2)/2.130(2)	2.599(2)/2.476(2)
P–M–N	83.13(7)	82.82(5)/83.33(5)	71.95(6)/74.50(6)
P–M–P′	125.12(4)	124.23(3)	139.41(2)
N–M–N′	111.48(9)	111.97(7)	101.98(8)
P–M–N′	129.68(7)	127.53(6)/132.49(6)	139.65(6)/132.25(5)
τ_4	0.71	0.71	0.57
N–C2–C3–P	7.1(4)	−4.2(3)/−7.9(3)	−4.9(3)/−9.8(3)
C1–N1	1.332(4)	1.330(3)/1.332(3)	1.310(4)/1.307(4)
C1–N2	1.353(4)	1.350(3)/1.349(3)	1.357(4)/1.353(4)
C1–N3	1.346(5)	1.357(3)/1.354(3)	1.369(4)/1.378(4)

[a] P–M–N is the angle pertaining to the chelating phosphinoguanidine ligand (bite angle), whereas P–M–N′ is the corresponding "open" angle, where the P and N atoms belong to the different ligands. [b] The molecule resides on the crystallographic two-fold axis, and hence, only its half is structurally independent.

the ideal tetrahedral values (102–112°), while the P–M–P′ and nonchelate P–M–N angles are significantly widened. The distortion of the coordination sphere is more pronounced in the Ag(I) complex than in its Cu(I) analogues that, in turn, differ only marginally. This can be illustrated by the τ_4 index,[10] which is 0.71 for both Cu(I) complexes and 0.57 for **3a** (*N.B.* ideal tetrahedral and planar coordination would yield τ_4 = 1 and 0, respectively) and by the angle subtended by the {M,P,N} planes of the two chelate rings, which is 78.5(1)° in **2a**, 78.23(8)° in **2b**, and 67.22(9)° in **3a** (in a regular tetrahedron, these planes would be perpendicular).

No significant torsion is observed at the central benzene ring, as evidenced by the N–C2–C3–P torsion angles (Table 1). The guanidine moieties are planar and partly delocalised: the C–N1 distance involving the coordinated nitrogen atom is consistently shorter than the remaining C–N bonds. The NH groups in **2a** and **2b** are *syn* and directed away from the central atom, while those in **3a** assume mutually *anti*-positions. These differences can be ascribed to hydrogen-bond interactions (see the ESI†).

Au(I) complexes

Au(I) complexes were obtained through reactions of **1** with Au(I) precursors with labile sulfide ligands (Scheme 3). Thus, the replacement of dimethylsulfide in [AuCl(SMe_2)] with **1** (Au : **1** = 1 : 1) produced the chlorogold(I) complex [AuCl(**1**-κ*P*)] (**4**), whereas the reaction with [Au(tht)$_2$][SbF_6] (Au : **1** = 1 : 2, tht = tetrahydrothiophene) gave the bis-phosphine complex [Au(**1**-κ*P*)$_2$][SbF_6] (**5**). Subsequent halogen removal using Ag[SbF_6] in MeCN cleanly converted the former compound into the dinuclear complex [{μ(P,N)-**1**}$_2$$Au_2$][$SbF_6$]$_2$ (**6**) rather than a solvent complex (*e.g.*, [Au(**1**-κ*P*)(MeCN)][SbF_6]). The preferred formation of **6** can be explained by a stabilising effect of the aurophilic interaction[11] in its structure (*vide infra*).

In view of subsequent catalytic testing, Au(I) complexes were also prepared using the protonated ligand **1**·HCl. The protonation expectedly prevented the coordination of the guanidine moiety: the reaction of [AuCl(SMe_2)] with **1**·HCl yielded the phosphine complex [AuCl(**1**H-κ*P*)]Cl (**7a**), which reacted with Ag[SbF_6] (1 equiv.) under anion exchange to give [AuCl(**1**H-κ*P*)][SbF_6] (**7b**).

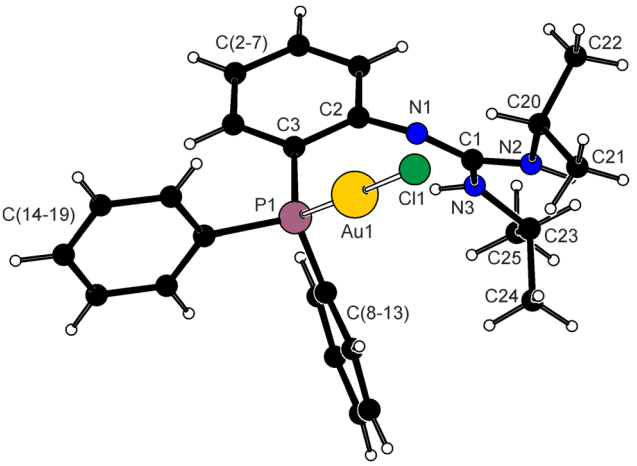

Fig. 2 The molecular structure of **4**.

Complexes **4**–**7** were characterised using NMR spectroscopy, ESI MS and elemental analysis. The ^{1}H NMR and ^{13}C NMR spectra displayed the expected signals but are difficult to compare because different solvents had to be used to dissolve the compounds. The ^{31}P NMR signals appeared downfield compared to the free ligand and their position depends on the other ligand in gold ($\delta_P \approx$ 24–25 for **4**, **6** and **7a**/**b**, and $\delta_P \approx$ 37 for **5**; in different solvents). The ESI MS of **4** and **7a**/**b** displayed ions attributable to AuCl(**1**H)$^+$ (*m*/*z* 636), while for **5** and **6**, signals due to Au(**1**)$_2^+$ were observed at *m*/*z* 1003.

The molecular structure of **4** is shown in Fig. 2 (the structures of solvated **7a** and **7a** are presented in the ESI†); Table 2 contains the relevant structural parameters.

The Au(I) ions in **4** and solvated **7a** and **7b** present typical linear coordination with parameters similar to those of [AuCl(PPh_3)].[12] In all structures, the linear P–Au–Cl moieties are bent out of the plane of the ligand's 1,2-phenylene backbone (*cf.* C2–C3–P–Au angles in Table 2), which is somewhat twisted in **4** (*N.B.* **7a** and **7b** show smaller N–C2–C3–P torsion angles). The guanidine moieties in **4** and **7a** are essentially

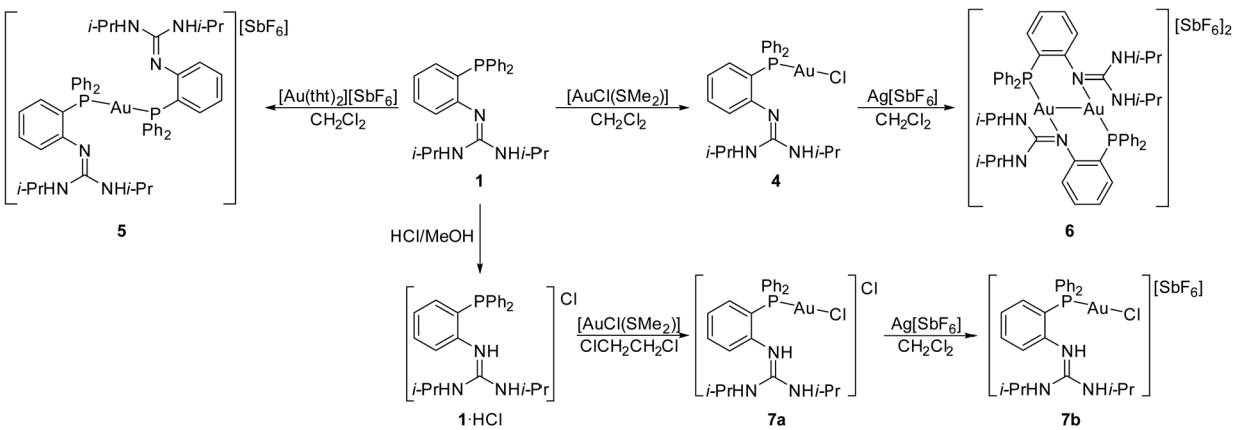

Scheme 3 Synthesis of Au(I) complexes **6**–**10** (tht = tetrahydrothiophene).

Table 2 Selected distances and angles for **4**, **7a**·H_2O·CH_2Cl_2 and **7b**·$\frac{1}{2}C_2H_4Cl_2$ (in Å and deg)

Parameter	**4**	**7a**·H_2O·CH_2Cl_2	**7b**·$\frac{1}{2}C_2H_4Cl_2$
Au–P	2.2287(5)	2.2276(7)	2.2279(8)
Au–Cl	2.2960(6)	2.2821(7)	2.2968(9)
P–Au–Cl	178.84(2)	176.35(3)	177.38(3)
C1–N1	1.301(2)	1.358(3)	1.355(4)
C1–N2/N3	1.356(2)/1.366(2)	1.335(3)/1.321(3)	—[a]
N–C2–C3–P	−11.7(2)	−3.6(3)	−4.8(4)
C2–C3–P–Au	50.1(1)	59.4(2)	57.9(3)

[a] The guanidine moiety is disordered, which particularly affects these distances.

planar with *anti*-positioned NH moieties and show differentiated C–N bonds: in **4**, the C1–N1 bond is shorter than the C1–N2/3 bonds, while the opposite is observed for **7a** with a protonated guanidine moiety. The orientation of the guanidine moiety towards the phenylene plane changes with intermolecular interactions, the lack of which can result in disorders such as in **7b** (see the ESI;† the dihedral angles of the C(2–7) and {C1,N1,N2,N3} planes are 67.97(9)° in **4** and 84.7(1)° in **7a**).

The gold atom in the structure of **5** also shows linear coordination (Fig. 3). The Au–P bond lengths are similar to those in $[Au(PPh_3)_2]X$ (X = SbF_6, PF_6 and BF_4)[13] and are elongated with respect to **4** due to a strong *trans* influence of the phosphine ligands,[14] which destabilise each other.[15] Steric factors may also play some role, as the ligands are oriented so that the P-bound phenyl groups and guanidine moieties from the two ligands are oriented towards each other (*syn*).

Complex **6** (Fig. 4) crystallised as a dichloromethane solvate, **6**·$2CH_2Cl_2$, with the $[\{\mu(P,N)\text{-}\mathbf{1}\}_2Au_2]^{2+}$ cations residing over the crystallographic inversion centres (space group $P2_1/n$). The structure of the complex cation is stabilised by intramolecular

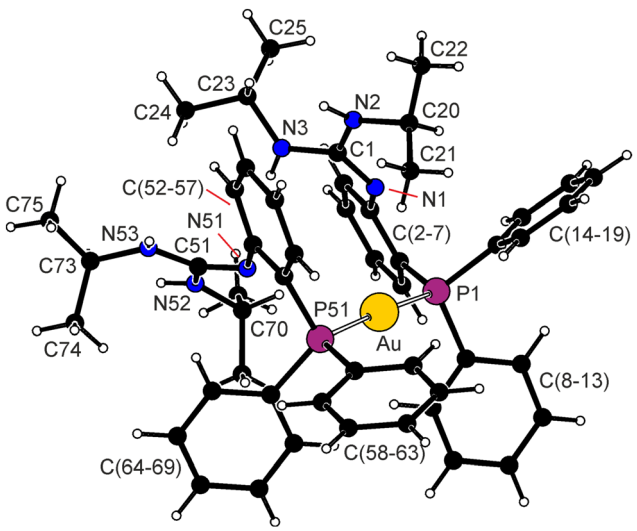

Fig. 3 View of the complex cation in the structure of **5**. The selected distances and angles for ligand **1** [ligand **2**] (in Å and deg): Au–P 2.3007(6) [2.3035(6)], P–Au–P 175.84(3), C1–N1 1.315(2) [1.304(2)], C1–N1 1.353(2) [1.357(2)], C1–N3 1.367(3) [1.357(2)], N1–C1–N2 118.9(2) [119.6(2)], N1–C1–N3 125.4(2) [124.2(2)], N2–C1–N3 115.6(2) [116.2(2)], N1–C2–C3–P 2.6(2).

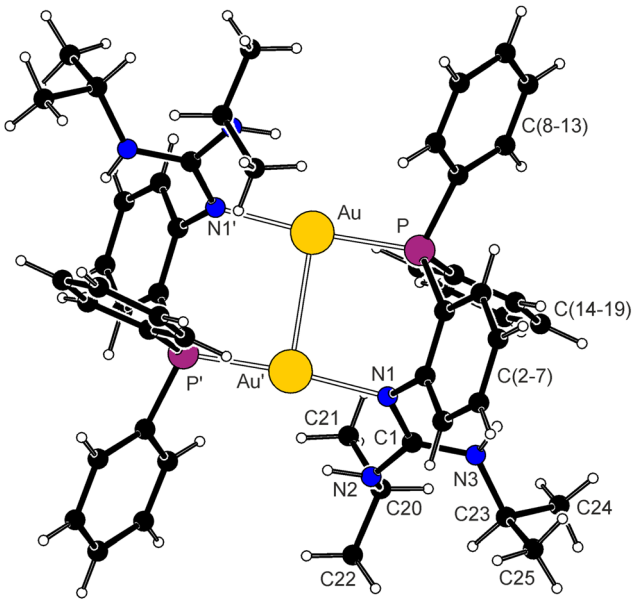

Fig. 4 View of the complex cation in the structure of **6**·$2CH_2Cl_2$. Selected distances and angles (in Å and deg): Au–Au′ 2.9003(4), Au–P 2.2491(8), Au–N′ 2.072(2), P–Au–N′ = 174.77(7), C1–N1 1.340(3), C1–N2 1.358(3), C1–N3 1.336(3), N1–C2–C3–P 1.9(3).

aurophilic interactions (Au–Au′ ≈ 2.90 Å), resulting in a slight inclination of the gold centres and bending of the P–Au–N moiety (175°). The Au–P bond length is similar to the value determined for **4** (*trans* influences of Cl^- and N-donors are similar), and the Au–N distance compares to the values reported for similar cationic dimers obtained from 2-(diphenylphosphino)-1-methylimidazole[16] and 2-(diphenylphosphino)-1-methylbenzimidazole.[17] The guanidine moiety is planar (within 0.002 Å) and the guanidine C–N bonds differ less than in the previously discussed structures (both NH groups are oriented towards the pivotal atom N1). The guanidine plane is twisted by 70.9(2)° from the plane of the 1,2-phenylene ring C(2–7), which diverts by 47.9(1)° from the plane of the central $\{Au_2P_2N_2\}$ moiety. Due to the imposed symmetry, the complex cation adopts an *anti*-arrangement, such that the phenylene ring from one ligand and the guanidine unit and one P-bound phenyl ring from the other are located on one side of the $\{Au_2P_2N_2\}$ ring.

Catalysis

The catalytic properties of the prepared gold(I) complexes were first evaluated using gold-mediated cyclisation of *N*-propargylbenzamide (**8**) into 5-methylene-2-phenyl-4,5-dihydrooxazole (**9**; Scheme 4).[18] The reaction, performed[19] in CD_2Cl_2 at 25 °C using 1 mol% of the gold catalyst, proceeded selectively, producing **9** as the only

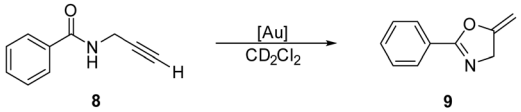

8 **9**

Scheme 4 Au-catalysed cyclisation of *N*-propargylbenzamide (**8**).

detectable product. As such, it was easily followed *in situ* by ^{1}H NMR spectroscopy.

The results collected in Table 3 illustrate the markedly different catalytic activities of complexes **4**–**7**, which were used without any promotor (*e.g.*, silver salt to abstract the chloride ligand). Compounds **4**, **5** and **7b** did not show any appreciable catalytic activity (<1% yield after 6 h), and complexes **6** and **7a** reacted only very slowly. Eventually, a fast-reacting catalyst was obtained upon adding bis(trifluoromethanesulfonyl)imide ($HNTf_2$)[20] to complex **6**. One equiv. of $HNTf_2$ per gold atom markedly accelerated the reaction but better yields at shorter reaction times were obtained with 2 equiv. of the acid. Addition of more than 2 equiv. of $HNTf_2$ per the gold atom had no beneficial effect.

In contrast to analogous complexes with P,N-bridging phosphinonitrile ligands,[21] complex **6** does not dissociate spontaneously under the reaction conditions. However, the addition of $HNTf_2$ to **6** leads to the protonation of the strongly basic guanidine moiety and, consequently, the cleavage of the dimeric structure into coordinatively unsaturated and catalytically active species $Au(\mathbf{1H})^+$ or their anion-stabilised form $[Au(\mathbf{1H})(NTf_2)]$. The activity of the formed species is comparable to that of species resulting from the spontaneous dissociation of $[Au_2L_2]^{2+}$ cations, which contain bridging ferrocene-based phosphinonitrile ligands and the prototypical gold(I) catalyst $[Au(PPh_3)(MeCN)][SbF_6]$.[19]

Catalyst activation was further followed by NMR titration: the addition of $HNTf_2$ to a solution of **6** in acetone-d_6 resulted in the gradual appearance of another set of signals (illustrated in Fig. 5 for the $CHMe_2$ signals and the ^{31}P NMR resonances), which cleanly replaced the signals due to **6**. The ^{31}P NMR signal of the new species shifted slightly upfield ($\delta_P \approx 20$).

The easy activation and high reactivity of the formed species led us to further consider complex **6** as an instant, silver-free gold precatalyst for reactions with acidic substrates that may activate the gold complex *in situ*. To demonstrate such applications, we performed additional reaction tests including the challenging gold-catalysed addition of benzoic acids across terminal alkynes to produce enol esters[22] (Scheme 5, results in Table 4).

Indeed, the model reaction between benzoic acid (**10a**) and 1-octyne (**11**) in 1,2-dichlorethane at 80 °C in the presence of 5 mol% of complex **6** proceeded selectively and gave a 40% yield of the Markovnikov addition product **12a** (with no other isomers detected). In contrast, no reaction occurred when using compounds **4**, **5**, **7a** and **7b** under similar conditions and even with complex **6** when the reaction solvent was changed to MeCN and 1,4-dioxane.

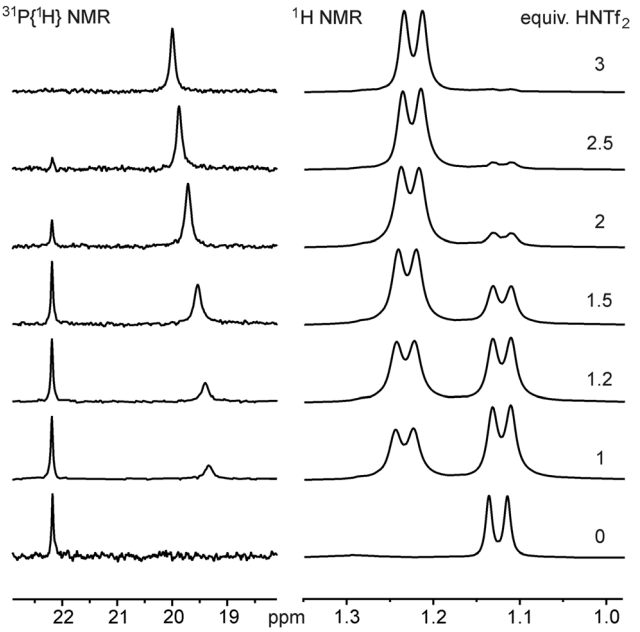

Fig. 5 Changes in the ^{31}P{^{1}H} and ^{1}H NMR spectra (region of $CHMe_2$ protons) of complex **6** after adding various amounts of $HNTf_2$ (recorded in $CDCl_3$ at 25 °C). The amount of $HNTf_2$ is given in molar equivalents per one gold atom.

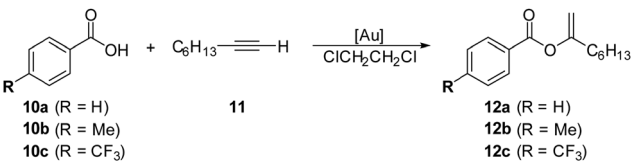

Scheme 5 Au-catalysed addition of benzoic acids across 1-octyne.

Table 3 Summary of the catalytic results achieved with complexes **4**–**7** in Au-catalysed cyclisation of amide **8** at different reaction times[a]

	Yield of **9** [%]		
Catalyst	1 h	3 h	6 h
4	0	0	0
5	0	0	0
6	4	6	10
6 + $HNTf_2$	44	89	100
6 + 2$HNTf_2$	48	99	100
6 + 3$HNTf_2$	43	99	100
6 + 3$HNTf_2$	40	99	100
7a	3	8	14
7b	0	0	0

[a] The reaction was performed in CD_2Cl_2 (c(**8**) = 0.25 M) at 25 °C using 1 mol% Au. $HNTf_2$ was added in the form of a freshly prepared stock solution in CD_2Cl_2. The amount of $HNTf_2$ is given in molar equivalents per gold atom.

Table 4 Summary of catalytic results achieved in the Au-catalysed addition of benzoic acids across 1-octyne[a]

	Yield of **12** [%]		
Acid	3 h	6 h	18 h
10a	13	26	40
10b	13	16	25
10c	23	33	45

[a] The reaction was performed in 1,2-dichloroethane at 80 °C (c(**10**) = c(**11**) = 0.3 M) using 5 mol% of the gold catalyst (*i.e.*, 2.5 mol% of **6**).

The relatively weaker acid **10b** gave a lower yield of the respective addition product (**12b**: 25%), while a slight improvement was noted when using the stronger acid **10c** (**12c**: 45%). Such results correspond with the presumed mode of catalyst activation, for which stronger acids are expected to be more efficient.

Conclusion

In summary, the results reported here indicate a similar behaviour of Cu(I) and Ag(I) ions in reactions with ligand **1**. Both ions favour the formation of tetracoordinate bis-chelate cations of the type $[M(\mathbf{1}\text{-}\kappa^2P,N)_2]^+$, which were isolated from experiments performed at the 1:1 and 1:2 metal-to-ligand ratios and obtained from precursors containing both coordinating and weakly coordinating anions. In contrast, the tested gold(I) precursors afford discrete mononuclear Au(I)–**1** complexes with linearly coordinated gold centres. Nevertheless, removal of the halide ligand from [AuCl(**1**-κ*P*)] with $Ag[SbF_6]$ results in the formation of a dimeric cation $[\{\mu(P,N)\text{-}\mathbf{1}\}_2Au_2]^{2+}$, stabilised by intramolecular aurophilic interactions. This cation can be cleaved through the action of Brønsted acids that protonate the guanidine moiety, thereby preventing its coordination. The resulting species, presumably $Au(\mathbf{1}H)^+$, are highly catalytically active. As such, complex **6** represents an attractive silver-free gold catalyst[23] that eliminates the possible interference of silver species arising from silver salts typically used to activate LAuCl-type precatalysts, which may also be catalytically active or can hamper the reaction, *e.g.*, by forming Ag–Au species.[24] The protonated guanidine moiety can further increase the affinity of the $Au(\mathbf{1}H)^+$ species towards substrates *via* charge-supported hydrogen bond interactions.

Experimental

Materials and methods

All syntheses were performed under a dinitrogen atmosphere using conventional Schlenk techniques. Compounds **1**[7] and **8**[19] were prepared according to the literature procedure. Other starting materials were purchased from commercial suppliers (Sigma-Aldrich, Alfa-Aesar, TCI) and used without additional purification. Dry and deoxygenated dichloromethane was obtained using a PureSolv MD5 solvent purification system (Innovative Technology). Solvents used for chromatography and crystallisation were used as received (analytical grade, Lach-Ner, Czech Republic).

NMR spectra were recorded on a Varian UNITY Inova 400 spectrometer at 25 °C unless stated otherwise. Chemical shifts (δ in ppm) are expressed relative to internal $SiMe_4$ (^{1}H and ^{13}C) and to external 85% aqueous H_3PO_4 (^{31}P), all set to 0 ppm. Electrospray ionisation (ESI) mass spectra were measured on a Bruker Compact Q-TOF instrument using samples dissolved in HPLC-grade methanol. MALDI TOF mass spectra were obtained on a Bruker MALDI TOF/TOF Ultraflex instrument. Elemental analyses were performed on a PerkinElmer PE 2400 Series II CHNS/O Elemental Analyser. The amount of clathrated solvent was determined by ^{1}H NMR analysis.

Syntheses

Preparation of $[Cu(\mathbf{1}\text{-}\kappa^2P,N)_2][BF_4]$ (2a). A solution of ligand **1** (80.7 mg, 0.20 mmol) in dichloromethane (2 mL) was added to $[Cu(MeCN)_4][BF_4]$ (31.5 mg, 0.10 mmol) dissolved in the same solvent (2 mL). The resultant mixture was stirred in the dark for 30 min and evaporated under vacuum. The solid residue was redissolved in dichloromethane (≈0.5 mL) and added to cold pentane to precipitate the product. The mixture was allowed to stand at 5 °C for 3 h, and the separated solid was isolated by suction and dried under vacuum. Yield: 89 mg (93%), white powdery solid.

^{1}H NMR (400 MHz, CD_2Cl_2): δ 0.72 (d, $^3J_{HH}$ = 6.4 Hz, 24 H, CH*Me*$_2$), 3.55 (vq, J = 6.4 Hz, 4 H, C*H*Me$_2$), 4.86 (d, $^3J_{HH}$ = 8.3 Hz, 4 H, NH), 6.85–6.91 (m, 2 H, C_6H_4), 7.05 (dtdd, J = 8.2, 2.9, 1.1, 0.5 Hz, 2 H, C_6H_4), 7.19–7.40 (m, 24 H, 4 C_6H_4 + PPh_2). ^{13}C{^{1}H} NMR (101 MHz, CD_2Cl_2): δ 22.58 (s, 8 C, CH*Me*$_2$), 44.81 (s, 4 C, CHMe$_2$), 121.26 (vt, J_{PC} = 2 Hz, 2 C, CH C_6H_4), 121.50 (s, 2 C, CH C_6H_4), 125.07 (vt, J_{PC} = 20 Hz, 2 C, C–P C_6H_4), 129.07 (vt, J_{PC} = 5 Hz, 8 C, CH PPh_2), 130.16 (s, 4 C, CH^{para} PPh_2), 131.92 (s, 2 C, CH C_6H_4), 133.73–133.88 (m, 10 C, 2 CH C_6H_4 + 8 CH PPh_2), 155.66 (vt, J_{PC} = 12 Hz, 2 C, C–N C_6H_4), 160.55 (s, 2 C, C^{ipso} guanidine). ^{31}P{^{1}H} NMR (162 MHz, CD_2Cl_2): δ −17.8 (br s). ESI+ MS: *m*/*z* 869 ([M − BF_4]$^+$), 420 ([**1**O + H]$^+$), 404 ([**1** + H]$^+$). Anal. calcd for $C_{50}H_{60}BCuF_4N_6P_2$ (957.37): C 62.73, H 6.32, N 8.78%. Found: C 62.63, H 6.15, N 8.41%.

Preparation of $[Ag(\mathbf{1}\text{-}\kappa^2P,N)_2][SbF_6]$ (3a). A dichloromethane solution of ligand **1** (40 mg, 0.10 mmol) was added to a mixture of $Ag[SbF_6]$ (17.2 mg, 0.050 mmol) and dichloromethane (2 mL) in a test tube. The mixture was magnetically stirred in the dark for 5 min and then layered with cyclohexane and set aside for crystallisation by slow liquid-phase diffusion. The crystals that separated over several days were filtered off, washed with cold pentane and dried under vacuum. Yield: 40 mg (70%), colourless crystals.

^{1}H NMR (400 MHz, CD_2Cl_2): δ 0.73 (d, $^3J_{HH}$ = 6.3 Hz, 24 H, CH*Me*$_2$), 3.60 (d of sept, $^3J_{HH}$ = 7.8, 6.5 Hz, 4 H, C*H*Me$_2$), 3.74 (d, $^3J_{HH}$ = 8.1 Hz, 4 H, NH), 6.95–7.02 (m, 6 H, C_6H_4), 7.38–7.52 (m, 22 H, 2 C_6H_4 + PPh_2). ^{13}C{^{1}H} NMR (101 MHz, CD_2Cl_2): δ 22.05 (s, 8 C, CHMe$_2$), 44.09 (s, 4 C, *C*HMe$_2$), 122.27 (vt, J_{PC} = 3 Hz, 2 C, CH C_6H_4), 123.64 (vt, J_{PC} = 2 Hz, 2 C, CH C_6H_4), 125.05 (vt, J_{PC} = 22 Hz, 2 C, C–P C_6H_4), 129.55 (vt, J_{PC} = 5 Hz, 8 C, CH PPh_2), 131.24 (s, 4 C, CH^{para} PPh_2), 131.80 (vt of doublets, J_{PC} = 16 Hz, $^2J_{AgC}$ = 5 Hz, 4 C, C^{ipso} PPh_2), 132.53 (s, 2 C, CH C_6H_4), 133.56 (vt of doublets, $J_{PC} \approx J_{AgC} \approx$ 1.5 Hz, 2 C, CH C_6H_4), 134.42 (vt of doublets, J_{PC} = 9 Hz, $^3J_{AgC}$ = 2 Hz, 8 C, CH^{ortho} PPh_2), 153.50 (vt of doublets, J_{PC} = 8 Hz, $^2J_{AgC}$ = 1 Hz, 2 C, C–N C_6H_4), 154.93 (s, 2 C, C^{ipso} guanidine). ^{31}P{^{1}H} NMR (162 MHz. CD_2Cl_2): δ −5.5 (pair of concentric doublets, $^1J_{AgP}$ = 503 (^{109}Ag), 436 (^{107}Ag) Hz). MALDI TOF: *m*/*z* 913 ([M − SbF_6]$^+$), 510 ([M − **1** − SbF_6]$^+$). Anal. calcd for $C_{50}H_{60}AgF_6N_6P_2Sb$ (1150.64): C 52.19, H 5.26, N 7.30%. Found: C 52.18, H 5.09, N 7.36%.

Preparation of $[Cu(\mathbf{1}\text{-}\kappa^2P,N)_2]Br$ (2b). A solution of ligand **1** (40 mg, 0.10 mmol) in dichloromethane (1 mL) was added to a

suspension of CuBr (7.2 mg, 0.050 mmol) in the same solvent (2 mL) in a test tube. The mixture was stirred for 20 min, whereupon all solids dissolved. The solution was evaporated, and the residue was dried under vacuum to give **2b**·0.2CH_2Cl_2 as a white solid. Yield: 41.4 mg (85%).

ESI+ MS: *m*/*z* 869 ([M – Br]$^+$), 466 ([M – **1** – Br]$^+$), 420 ([**1**O + H])$^+$, 404 ([**1** + H])$^+$. Anal. calcd for $C_{50}H_{68}BrCuN_6P_2$·0.2CH_2Cl_2 (975.50): C 62.32, H 6.29, N 8.69%. Found: C 62.41, H 6.62, N 8.23%. The NMR spectra could not be acquired because the compound is insoluble in nonpolar and moderately polar deuterated solvents and decomposes in strongly polar solvents.

Preparation of [Ag(1-κ^2*P*,*N*)$_2$]Br (3b). Ligand **1** (40.4 mg, 0.10 mmol) and finely powdered AgBr (9.4 mg, 0.050 mmol) were mixed in 1,2-dichloroethane (5 mL), and the mixture was stirred in the dark overnight. Then, it was filtered through a 0.45 μm PTFE syringe filter, and the filtrate was layered with cyclohexane (approximately 15 mL). The mixture was allowed to crystallise in the dark by liquid-phase diffusion over several days. The separated microcrystalline solid was filtered off and dried under vacuum. Yield of **3b**·C_6H_{12}: 34 mg (68%), white solid.

ESI+ MS: *m*/*z* 995 ([M + H]$^+$), 915 ([M – Br]$^+$), 404 ([L + H]$^+$). Anal. calcd for $C_{50}H_{60}AgBrN_6P_2$·C_6H_{12} (1078.95): C 62.34, H 6.73, N 7.79%. Found: C 61.78, H 6.39, N 7.63%. The compound is virtually insoluble in common deuterated solvents, which precluded recording the NMR spectra.

Synthesis of [AuCl(1-κ*P*)] (4). [AuCl(SMe_2)] (294.6 mg, 1.0 mmol) and ligand **1** (403.5 mg, 1.0 mmol) were dissolved in dichloromethane (10 mL), and the solution was stirred overnight before evaporation under vacuum. The residue was dissolved in dichloromethane (approximately 3 mL), and the solution was added to a pentane/diethyl ether mixture (1 : 1, 25 mL). The resultant mixture was stored at 4 °C for 3 h, whereupon it deposited a crystalline solid, which was isolated by suction filtration, washed with pentane and dried under vacuum. Yield: 564 mg (88%), colourless, needle-like crystals.

^{1}H NMR (400 MHz, $CDCl_3$): δ 1.04 (d, $^3J_{HH}$ = 6.4 Hz, 12 H, $CHMe_2$), 3.57 (d of sept, $^3J_{HH}$ = 7.7, 6.5 Hz, 2 H, C*H*Me_2), 3.82 (d, $^3J_{HH}$ = 7.4 Hz, 2 H, NH), 6.65 (ddd, *J* = 11.8, 7.8, 1.4 Hz, 1 H, C_6H_4), 6.82 (ddt, *J* = 7.7, 2.4, 1.1 Hz, 1 H, C_6H_4), 6.96 (ddd, *J* = 8, 5.2, 0.7 Hz, 1 H, C_6H_4), 7.36–7.61 (m, 11 H, 1 C_6H_4 + PPh_2). ^{13}C{^{1}H} NMR (101 MHz, $CDCl_3$): δ 23.61 (s, 4 C, CH*Me*$_2$), 43.12 (s, 2 C, *C*HMe_2), 120.26 (d, J_{PC} = 10 Hz, 1 C, CH C_6H_4), 121.63 (d, $^1J_{PC}$ = 71 Hz, 1 C, C–P C_6H_4), 121.95 (d, J_{PC} = 6 Hz, 1 C, CH C_6H_4), 128.62 (d, J_{PC} = 12 Hz, 4 C, CH PPh_2), 130.16 (d, $^1J_{PC}$ = 63 Hz, 2 C, C^{ipso} PPh_2), 130.95 (d, $^4J_{PC}$ = 2 Hz, 2 C, CH^{para} PPh_2), 132.77 (d, J_{PC} = 2 Hz, 1 C, CH C_6H_4), 133.70 (d, J_{PC} = 8 Hz, 1 C, CH C_6H_4), 149.13 (s, 1 C, C^{ipso} guanidine), 153.95 (d, $^2J_{PC}$ = 8 Hz, 1 C, C–N C_6H_4). ^{31}P{^{1}H} NMR (161.90 MHz, $CDCl_3$): δ 26.2 (s). ESI+ MS: *m*/*z* 636 ([M + H]$^+$). Anal. calcd for $C_{25}H_{30}AuClN_3P$ (635.93): C 47.22, H 4.76, N 6.61%. Found: C 47.29, H 4.58, N 6.90%.

Synthesis of [Au(1-κ*P*)$_2$][SbF_6] (5). Solid [Au(tht)$_2$][SbF_6] (30.5 mg, 0.050 mmol) and ligand **1** (40 mg, 0.10 mmol) were dissolved in dichloromethane (10 mL), and the mixture was stirred for 30 min. Subsequent evaporation produced a white solid residue, which was sonicated twice with diethyl ether (2 mL) to efficiently remove tetrahydrothiophene and finally dried under vacuum to give **5** as a white solid. Yield: 50.2 mg (82%).

^{1}H NMR (400 MHz, $CDCl_3$): δ 0.75 (d, $^3J_{HH}$ = 6.3 Hz, 24 H, CH*Me*$_2$), 3.59 (sept, $^3J_{HH}$ = 6.9 Hz, 4 H, C*H*Me_2), 3.73 (d, $^3J_{HH}$ = 7.9 Hz, 4 H, NH), 6.71 (dtd, *J* = 7.2, 5.6, 1.5 Hz, 2 H, C_6H_4), 6.87 (dtd, *J* = 7.6, 2.5, 1.3 Hz, 2 H, C_6H_4), 7.03 (dtd, *J* = 8.2, 2.8, 0.6 Hz, 2 H, C_6H_4), 7.42–7.60 (m, 22 H, 2 C_6H_4 + PPh_2). ^{13}C{^{1}H} NMR (101 MHz, $CDCl_3$): δ 23.05 (s, 8 C, CH*Me*$_2$), 42.84 (s, 4 C, *C*HMe_2), 120.57 (vt, J_{PC} = 5 Hz, 2 C, CH C_6H_4), 121.61 (broad t, 2 C, CH C_6H_4), 121.69 (vt, J_{PC} = 34 Hz, C–P C_6H_4), 129.15 (vt, J_{PC} = 6 Hz, 8 C, CH PPh_2), 129.83 (vt, J_{PC} = 30 Hz, 4 C, C^{ipso} PPh_2), 131.58 (s, 4 C, CH^{para} PPh_2), 133.30 (s, 2 C, CH C_6H_4), 133.76 (vt, J_{PC} = 4 Hz, CH C_6H_4), 133.99 (vt, J_{PC} = 8 Hz, 8 C, CH PPh_2), 150.12 (s, 2 C, C^{ipso} guanidine), 153.69 (vt, J_{PC} = 5 Hz, 2 C, C–N C_6H_4). ^{31}P{^{1}H} NMR (161.90 MHz, $CDCl_3$): δ 37.4 (s). ESI+ MS: *m*/*z* 1003 ([M – SbF_6]$^+$). Anal. calcd for $C_{50}H_{60}AuF_6N_6P_2Sb$ (1239.72): C 48.44, H 4.88, N 6.78%. Found: C 48.58, H 4.91, N 6.68%.

Preparation of [{μ(P,N)-1}$_2$Au$_2$][SbF_6]$_2$ (6). Complex **4** (318 mg, 0.50 mmol) was dissolved in dichloromethane (7 mL), and the solution was added dropwise to an acetonitrile solution of Ag[SbF_6] (172 mg, 0.50 mmol in 3 mL of the solvent). A white precipitate (AgCl) formed immediately. The mixture was stirred in the dark for 30 min and filtered through a PTFE syringe filter (0.45 μm pore size). The filtrate was evaporated under vacuum, and the orange solid residue was redissolved in dichloromethane (approximately 3 mL). The solution was treated with a small amount of charcoal (10 mg) and filtered through a Celite pad using a syringe filter. The filtrate was added directly into a pentane/diethyl ether mixture (1 : 1, 25 mL), whereupon a white solid was deposited. The mixture was stored at 4 °C for 18 h before the solid was collected on a glass frit and dried under vacuum to give **6** as a white solid. Yield: 285 mg (68%).

^{1}H NMR (400 MHz, acetone-d_6): δ 1.12 (d, $^3J_{HH}$ = 6.4 Hz, 24 H, CH*Me*$_2$), 4.16 (br s, 4 H, C*H*Me_2), 5.53 (br s, 4 H, NH), 6.86 (ddd, *J* = 12.8, 7.9, 1.5 Hz, 2 H, C_6H_4), 7.36 (dddd, *J* = 15.3 ≈ 15.3, 1.5 ≈ 1.4 Hz, 2 H, C_6H_4), 7.61 (ddd, *J* = 8.0, 5.0, 1.2 Hz, 2 H, C_6H_4), 7.65–7.88 (m, 22 H, 2 HC_6H_4 + 20 H, PPh_2). ^{13}C{^{1}H} NMR (101 MHz, acetone-d_6): δ 23.37 (s, 8 C, CH*Me*$_2$), 47.09; 47.18 (d, J_{PC} = 9 Hz, *C*HMe_2), 125.65 (d, $^1J_{PC}$ = 65 Hz, 2 C, C–P C_6H_4), 127.84 (d, J_{PC} = 10 Hz, 2 C, CH C_6H_4), 128.06 (d, $^1J_{PC}$ = 66 Hz, 4 C, C^{ipso} PPh_2), 130.29 (filled d, *J* = 6 Hz, 2 C, CH C_6H_4), 130.83 (filled d, *J* = 13 Hz, 8 C, CH PPh_2), 133.88 (vt, *J*′ = 1 Hz, CH^{para} PPh_2), 135.37 (filled d, *J* = 15 Hz, 8 C, CH PPh_2), 135.44 (s, 2 C, CH C_6H_4), 135.74 (d, J_{PC} = 7 Hz, 2 C, CH C_6H_4), 148.67 (d, $^2J_{PC}$ = 5 Hz, C–N C_6H_4), 158.76 (d, $^4J_{PC}$ = 5 Hz, C^{ipso} guanidine). ^{31}P{^{1}H} NMR (162 MHz, acetone-d_6): δ 23.84 (s). ESI+ MS: *m*/*z* 1003 (Au(**1**)$_2^+$). Anal. calcd for: $C_{50}H_{60}Au_2F_{12}N_6P_2Sb_2$ (1672.45): C 35.91, H 3.62, N 5.03%. Found: C 35.78, H 3.45, N 4.77%.

Synthesis of [AuCl(1H-κ*P*)]Cl (7a). [AuCl(Me_2S)] (29.5 mg, 0.10 mmol) and hydrochloride **1**·HCl (44 mg, 0.10 mmol) were dissolved in 1,2-dichloroethane (5 mL) in a test tube. The

mixture was stirred for 5 min and then layered with cyclohexane. Crystallisation by liquid-phase diffusion produced crystals of solvated complex **7a**, which were filtered off, washed with diethyl ether and dried under vacuum. Yield of **7a**·H_2O·$C_2H_4Cl_2$: 70.6 mg (81%), colourless needles.

^{1}H NMR (400 MHz, acetone-d_6): δ 1.18 (d, $^3J_{HH}$ = 6.4 Hz, 12 H, $CHMe_2$), 4.03 (br s, 2 H, $CHMe_2$), 7.06 (dd, J = 11.5, 7.8 Hz, 1 H, C_6H_4), 7.50 (br t, J = 7.4 Hz, 1 H, C_6H_4), 7.56–7.68 (m, 11 H, 1 C_6H_4 + 10 PPh_2), 7.76 (br t, J = 7.4 Hz, 1 H, C_6H_4), 8.03 (br s, 2 H, NH), 9.97 (br s, 1 H, NH^+). ^{13}C{^{1}H} NMR (101 MHz, acetone-d_6): δ 23.18 (s, 4 C, $CHMe_2$), 46.38 (d, J_{PC} = 9 Hz, 2 C, $CHMe_2$), 129.25 (d, $^1J_{PC}$ = 64 Hz, 2 C, C^{ipso} PPh_2), 129.39 (d, J_{PC} = 10 Hz, 1 C, C_6H_4), 130.56 (d, J_{PC} = 12 Hz, 4 C, CH PPh_2), 133.16 (d, J_{PC} = 3 Hz, 2 C, CH^{para} PPh_2), 134.68 (d, J_{PC} =2 Hz, 1 C, C_6H_4), 135.33 (d, J_{PC} = 14 Hz, 4 C, CH PPh_2), 135.87 (d, J_{PC} = 6 Hz, 1 C, C–N C_6H_4), 140.84 (s, 1 C, C_6H_4), 154.99 (s, 1 C, C^{ipso} guanidine). The signal due to C–P C_6H_4 was not observed. ^{31}P{^{1}H} NMR (162 MHz, acetone-d_6): δ 24.72 (s). ESI+ MS: m/z 636 ([M – Cl]$^+$). Anal. calcd for $C_{25}H_{31}AuCl_2N_3P$·H_2O·$C_2H_4Cl_2$ (789.35): C 41.08, H 4.72, N 5.32%. Found: C 40.73, H 4.27, N 5.21%.

Synthesis of [AuCl(1H-κ*P*)][SbF_6] (7b). A solution of complex **7a** (67.2 mg, 0.10 mmol) in dichloromethane (2 mL) was added to a suspension of Ag[SbF_6] (34.4 mg, 0.10 mmol) in 3 mL of dichloromethane. A white precipitate formed instantly. The mixture was stirred in the dark for 30 min and filtered through a PTFE syringe filter (0.45 μm porosity), and the filtrate was evaporated under vacuum. The residue was taken up with dichloromethane (1 mL) and precipitated by adding into a pentane/diethyl mixture (1 : 1, 20 mL). After the separated solid was aged at 4 °C for 18 h, the solvent was poured away (decantation), and the residue was dried under vacuum to give **7b** as a white powdery solid. Yield: 84 mg (96%).

^{1}H NMR (400 MHz, CD_2Cl_2): δ 1.21 (d, $^3J_{HH}$ = 6.2 Hz, 12 H, $CHMe_2$), 3.63 (vq, J = 6.2 Hz, 2 H, $CHMe_2$), 5.25 (br, 2 H, NH), 6.73 (br, 1 H, NH^+), 7.00 (dd, J = 11.4, 7.6 Hz, 1 H, C_6H_4), 7.53 (vt, J = 7.4 Hz, 1 C, C_6H_4), 7.56–7.70 (m, 11 H, C_6H_4 + 10 PPh_2), 7.80 (vt, J = 7.4 Hz, 1 H, C_6H_4). ^{13}C{^{1}H} NMR (101 MHz, CD_2Cl_2): δ 22.79 (s, 4 C, $CHMe_2$), 46.23 (s, 2 C, $CHMe_2$), 126.32 (d, $^1J_{PC}$ = 65 Hz, 2 C, C^{ipso} PPh_2), 130.55 (d and br s, J_{PC} = 12 Hz, 5 C, CH C_6H_4 + 4 CH PPh_2), 133.66 (d, $^4J_{PC}$ = 2 Hz, 2 C, CH^{para} PPh_2), 134.84 (d, J_{PC} = 14 Hz, 4 C, CH PPh_2), 135.06 (s, 1 C, CH C_6H_4), 135.50 (d, J_{PC} = 6 Hz, 1 C, CH C_6H_4), 139.29 (br s, 1 C, C–N C_6H_4), 152.10 (s, 1 C, C^{ipso} guanidine). The signals due to CH and C–P of C_6H_4 were not observed, presumably due to overlaps. ^{31}P{^{1}H} NMR (162 MHz, CD_2Cl_2): δ 24.21 (s). ESI+ MS: m/z 636 ([M – SbF_6]$^+$). Anal. calcd for $C_{25}H_{31}AuClF_6N_3PSb$ (872.68): C 34.41, H 3.58, N 4.82%. Found: C 34.56, H 3.39, N 4.55%.

Catalytic experiments

Cyclisation of *N*-propargyl benzamide (8). The appropriate Au complex (1 mol%) was dissolved in CD_2Cl_2 (0.8 mL), and the solution was added to substrate **8** (31.8 mg, 0.20 mmol). Note: the catalyst solution was prepared a day earlier and stored in a refrigerator overnight. If Tf_2NH was a component of the reaction mixture, it was added to the solution of the gold complex in the form of a freshly prepared stock solution in CD_2Cl_2 (*ca.* 10 mg mL^{-1}) using an automatic pipette (the total volume was kept at 0.8 mL).

The reaction mixture was transferred to an NMR tube and analysed by ^{1}H NMR spectroscopy at 25 °C after 1, 3 and 6 h of mixing. The conversion was determined by the integration of the NCH_2 signals due to substrate **8** (δ_H 4.21) and the cyclisation product 5-methylene-2-phenyl-4,5-dihydrooxazole (**9**; δ_H 4.63).[19] The reaction proceeded selectively; no other compounds were detected in the NMR spectra.

Addition of benzoic acid across 1-octyne. A pressure Schlenk tube was charged with benzoic acid (36.6 mg, 0.30 mmol), 1-octyne (44 μL, 0.30 mmol) and *p*-anisaldehyde (36.5 μL, 0.30 mmol) as an internal standard. The gold catalyst (5 mol% Au) was dissolved in 1,2-dichloroethane (1 mL), and the solution was introduced to a Schlenk tube, which was then transferred to an oil bath maintained at 80 °C. The reaction was monitored by ^{1}H NMR spectroscopy. Small aliquots (0.2 mL) were withdrawn after 3, 6 and 18 reaction times and diluted with dmso-d_6 (0.5 mL), and the yield was determined by comparing the signal due to the CH_2 group of the addition product (δ_P 4.85, $=CH_2$)[25] and the formyl group of the standard (δ_P 9.87, singlet). Reactions with different benzoic acids and in different solvents were performed similarly.

X-ray crystallography

The full-sphere diffraction data were recorded at 120 or 150 K using a Bruker D8 VENTURE Kappa Duo diffractometer equipped with a PHOTON III detector and a Cryostream Cooler (Oxford Cryosystems). Mo Kα radiation (λ = 0.71073 Å) was used in all cases. The structures were solved by direct methods (SHELXT-2014/2018[26]) and refined by a full-matrix least-squares routine based on F^2 (SHELXL-2017[27]). All nonhydrogen atoms were refined with anisotropic displacement parameters. The NH hydrogen atoms were located on the difference electron density map and refined as riding atoms with U_{iso}(H) = 1.2U_{eq}(N). Hydrogen atoms in the CH_n groups were placed in their theoretical positions and refined similarly using the standard parameters in SHELXL.

Compound **2a**·$C_2H_4Cl_2$ crystallised as a racemic twin (space group $C2$, refined contributions of the two enantiomeric domains were ≈94 : 6). One of the phenyl substituents had to be refined over two positions as an ideal hexagon due to disorder (occupancies: 71 : 29). In addition, the solvent in this structure was severely disordered within structural voids and, hence, was treated as a diffuse electron density using PLATON SQUEEZE.[28] A similar situation was encountered in **7a**·H_2O·CH_2Cl_2 and **7b**·$\frac{1}{2}C_2H_4Cl_2$. In the former compound, not only were the solvent molecules disordered but also the chloride anion and water molecule occupied the same positions with equal abundance. For the latter compound, the disorder also affected the guanidine moiety, which had to be refined over two positions.

Relevant crystallographic data and refinement parameters are available in the ESI† (Table S1). All geometric data and structural diagrams were obtained using a recent version of the

PLATON program.[29] The numerical values were rounded to one decimal place with respect to their estimated standard deviations.

Conflicts of interest

There are no conflicts to declare.

Acknowledgements

This work was supported by the Charles University Research Centre program (project no. UNCE/SCI/014).

Notes and references

1 T. S. Teets, J. A. Labinger and J. E. Bercaw, *Organometallics*, 2013, **32**, 5530.
2 (*a*) M. Carmona, J. Ferrer, R. Rodríguez, V. Passarelli, F. J. Lahoz, P. García-Orduña, L. Cañadillas-Delgado and D. Carmona, *Chem. – Eur. J.*, 2019, **25**, 13665; (*b*) A. Parker, P. Lamata, F. Viguri, R. Rodríguez, J. A. López, F. J. Lahoz, P. García-Orduña and D. Carmona, *Dalton Trans.*, 2020, **49**, 13601; (*c*) M. Carmona, R. Pérez, J. Ferrer, R. Rodríguez, V. Passarelli, F. J. Lahoz, P. García-Orduña and D. Carmona, *Inorg. Chem.*, 2022, **61**, 13149.
3 T. Šmejkal, D. Gribkov, J. Geier, M. Keller and B. Breit, *Chem. – Eur. J.*, 2010, **16**, 2470.
4 (*a*) K. Jess, V. Derdau, R. Weck, J. Atzrodt, M. Freytag, P. G. Jones and M. Tamm, *Adv. Synth. Catal.*, 2017, **359**, 629; (*b*) M. Valero, D. Becker, K. Jess, R. Weck, J. Atzrodt, T. Bannenberg, V. Derdau and M. Tamm, *Chem. – Eur. J.*, 2019, **25**, 6517.
5 O. Bárta, R. Gyepes, I. Císařová, A. Alemayehu and P. Štěpnička, *Dalton Trans.*, 2020, **49**, 4225.
6 O. Bárta, I. Císařová and P. Štěpnička, *Dalton Trans.*, 2021, **50**, 14662.
7 Z. Leitner, I. Císařová and P. Štěpnička, *New J. Chem.*, 2022, **46**, 1060.
8 W. H. Hersh, *J. Chem. Educ.*, 1997, **74**, 1485.
9 The metal-donor distances are comparable with those determined for phosphinoamine and phosphinooxazoline Cu(I) and Ag(I) complexes. For selected examples, see: (*a*) E. W. Ainscough, A. M. Brodie, S. L. Ingham and J. M. Waters, *Inorg. Chim. Acta*, 1994, **215**, 191; (*b*) P. Papathanasiou, G. Salem, P. Waring and A. C. Willis, *J. Chem. Soc., Dalton Trans.*, 1997, 3435; (*c*) W. Kaim, M. Wanner, A. Knodler and S. Zalis, *Inorg. Chim. Acta*, 2002, **337**, 163; (*d*) O. Bárta, M. Drusan, I. Císařová, R. Šebesta and P. Štěpnička, *New J. Chem.*, 2018, **42**, 11450; (*e*) R. Giereth, A. K. Mengele, W. Frey, M. Kloss, A. Steffen, M. Karnahl and S. Tschierlei, *Chem. – Eur. J.*, 2020, **26**, 2675.
10 L. Yang, D. R. Powell and R. P. Houser, *Dalton Trans.*, 2007, 955.
11 (*a*) H. Schmidbaur and A. Schier, *Chem. Soc. Rev.*, 2008, **37**, 1931; (*b*) H. Schmidbaur and A. Schier, *Chem. Soc. Rev.*, 2012, **41**, 370.
12 S. P. C. Dunstan, P. C. Healy, A. N. Sobolev, E. R. T. T. iekink, A. H. White and M. L. Williams, *J. Mol. Struct.*, 2014, **1072**, 253.
13 (*a*) F. Inagaki, C. Matsumoto, Y. Okada, N. Maruyama and C. Mukai, *Angew. Chem., Int. Ed.*, 2015, **54**, 818; (*b*) R. J. Staples, C. King, M. N. I. Khan, R. E. P. Winpenny and J. P. Fackler, Jr., *Acta Crystallogr., Sect. C: Cryst. Struct. Commun.*, 1993, **49**, 472; (*c*) J.-C. Wang, *Acta Crystallogr., Sect. C: Cryst. Struct. Commun.*, 1996, **53**, 611.
14 (*a*) T. G. Appleton, H. C. Clark and L. E. Manzer, *Coord. Chem. Rev.*, 1973, **10**, 335; (*b*) F. R. Hartley, *Chem. Soc. Rev.*, 1973, **2**, 163.
15 (*a*) R. G. Pearson, *Inorg. Chem.*, 1973, **12**, 712; (*b*) J. Vicente, A. Arcas, D. Bautista and P. G. Jones, *Organometallics*, 1997, **16**, 2127.
16 V. J. Catalano and S. J. Horner, *Inorg. Chem.*, 2003, **42**, 8430.
17 D. E. Jenkins and Z. Assefa, *J. Mol. Struct.*, 2017, **1133**, 374.
18 (*a*) A. S. K. Hasmi, J. P. Weyrauch, W. Frey and J. W. Bats, *Org. Lett.*, 2004, **6**, 4391; (*b*) J. P. Weyrauch, A. S. K. Hashmi, A. Schuster, T. Hengst, S. Schetter, A. Littmann, M. Rudolph, M. Hamzic, J. Visus, F. Rominger, W. Frei and J. W. Bats, *Chem. – Eur. J.*, 2010, **16**, 956.
19 O. Bárta, I. Císařová, J. Schulz and P. Štěpnička, *New J. Chem.*, 2019, **43**, 11258.
20 W. Zhao and J. Sun, *Chem. Rev.*, 2018, **118**, 10349.
21 K. Škoch, I. Císařová and P. Štěpnička, *Chem. – Eur. J.*, 2015, **21**, 15998.
22 (*a*) V. Cadierno, *Catalysts*, 2017, **7**, 328; (*b*) V. Cadierno, *Catalysts*, 2020, **10**, 1206.
23 H. Schmidbaur and A. Schier, *Z. Naturforsch.*, 2011, **66b**, 329.
24 For selected examples, see: (*a*) D. Weber and M. R. Gagné, *Org. Lett.*, 2009, **11**, 4962; (*b*) D. Wang, R. Cai, S. Sharma, J. Jirak, S. K. Thummanapelli, N. G. Akhmedov, H. Zhang, X. Liu, J. L. Petersen and X. Shi, *J. Am. Chem. Soc.*, 2012, **134**, 9012; (*c*) Z. Lu, J. Han, G. B. Hammond and B. Xu, *Org. Lett.*, 2015, **17**, 4534; (*d*) A. Franchino, M. Montesinos-Magraner and A. M. Echavarren, *Bull. Chem. Soc. Jpn.*, 2021, **94**, 732.
25 (*a*) C. D. Yi and R. Gao, *Organometallics*, 2009, **28**, 6585; (*b*) B. C. Chary and S. Kim, *J. Org. Chem.*, 2010, **75**, 7928.
26 G. M. Sheldrick, *Acta Crystallogr., Sect. A: Found. Adv.*, 2015, **71**, 3.
27 G. M. Sheldrick, *Acta Crystallogr., Sect. C: Struct, Chem.*, 2015, **71**, 3.
28 A. L. Spek, *Acta Crystallogr., Sect. C: Struct, Chem.*, 2015, **71**, 9.
29 (*a*) A. L. Spek, *J. Appl. Crystallogr.*, 2003, **36**, 7; (*b*) A. L. Spek, *Acta Crystallogr., Sect. D: Biol. Crystallogr.*, 2009, **65**, 148.

